Assessing the effectiveness of regional physical distancing measures of COVID-19 in rural regions of British Columbia

Geoffrey McGregor[1], Jennifer Tippett[2], Andy T.S. Wan*[1], Mengxiao Wang[3], and Samuel W.K. Wong[3]

[1]*Department of Mathematics and Statistics, University of Northern British Columbia, Prince George, Canada*
[2]*School of Health Sciences, University of Northern British Columbia, Prince George, Canada*
[3]*Department of Statistics and Actuarial Science, University of Waterloo, Waterloo, Canada*

April 18, 2021

Abstract

We study the effects of physical distancing measures for the spread of COVID-19 in regional areas within British Columbia, using the reported cases of the five provincial Health Authorities. Building on the Bayesian epidemiological model of [Anderson et al., 2020], we propose a hierarchical Bayesian model with time-varying regional parameters to account for the relative reduction in contact due to physical distancing and increased testing from March to December of 2020. In the absence of COVID-19 variants and vaccinations during this period, we examine the regionalized basic reproduction number, modelled prevalence, fraction of normal contacts, proportion of anticipated cases, and we observed significant differences between the provincial-wide and regional models.

1 Introduction

Coronavirus disease 2019 (COVID-19), caused by severe acute respiratory syndrome coronavirus 2 (SARS-CoV-2), was declared by the World Health Organization (WHO) to be a global pandemic on March 11, 2020. The virus and its associated illness have, in the past year, spread from their origin in Wuhan, China to nearly every corner of the world. The first reported case of COVID-19 arrived in the province of British Columbia (BC) in Canada on January 28, 2020 [The Canadian Press, 2021]. As of the one-year anniversary of the pandemic being declared by the WHO, March 11, 2021, BC has had 86,219 positive cases and 1,397 deaths [Government of Canada, 2021a].

Prior to the development of vaccines and with the currently on-going COVID-19 immunization plan, many countries around the world and their associated provinces, states, or subregions, including BC, have been relying on non-medical interventions to control the transmission of the virus. The application of these interventions — including mask-wearing, physical distancing, increased hand hygiene, travel restrictions, and putting limits on or banning social gatherings — can be either fixed or dynamic and is intended to prevent overwhelming the health care system. Fixed interventions are in place for a set duration of time and dynamic interventions are cycled on and off in response to the demand on the health care system. The latter can

*Author for correspondence. Email: andy.wan@unbc.ca

potentially be more effective at mitigating health care system strain, while concurrently providing the population with intermittent economic and psychological relief [Tuite et al., 2020]. However, the periods of tightening and relaxation of COVID-19 restrictions can have a dramatic effect on the number of new COVID-19 case incidences over time and the overall duration of the pandemic [Shafer et al., 2021]. Thus some countries, including New Zealand, have preferred a "COVID zero" approach where these non-medical interventions are strictly enforced with the goal being to completely eliminate COVID-19 infection within a specific geographic region, which goes farther than trying to control hospitalizations [McKee, 2020]. In contrast, BC has applied dynamic non-medical interventions to control the strain on the health care system. Although BC is in the midst of its COVID-19 immunization roll-out, vaccine supply issues from international suppliers and the vast task of inoculating every interested eligible resident of BC have prolonged the necessity of using non-medical interventions to reduce the spread of the virus.

Urban and rural areas, including those within BC, are heterogeneous regarding population density, cultural profile, the social determinants of health, and attitudes towards COVID-19 restrictions. According to the [OECD, 2020], 60% of Indigenous Canadians live in rural regions; therefore, there is a larger proportion of Indigenous people residing in rural versus urban areas of the country. Many rural areas fall behind urban regions when it comes to the social determinants of health. Specifically, there is an inherent lack of availability of health services in rural areas and there are significant geographical barriers to accessing health services [Garasia and Dobbs, 2019]. On average, rural residents have to travel four times farther than those in urban regions to visit a physician [Garasia and Dobbs, 2019]. Finally, non-medical interventions rely on the collective goodwill of the people to comply with public health orders and the perceived threat of COVID-19. These behaviours and perceptions are known to vary between urban and rural regions. Specifically, rural residents have been found to be less likely to adapt their behaviour in response to COVID-19 and to have more negative perceptions of the effectiveness of the non-medical interventions available to reduce COVID-19 [Chen and Chen, 2020]. While these significant differences of urban and rural areas persist, BC has seen predominantly blanketed restrictions across the province based on COVID-19 projections using data sourced from urban centres for the majority of 2020. Thus, macro-level modelling at the provincial or territorial level may be ignoring the nuances of rural living and limiting the specificity of these models to non-urban areas [Lavoie et al., 2016]. One metric utilized for quantifying these regional differences is the basic reproduction number, R_0, defined as the expected number of new cases a single infectious person will generate. For example, [Turk et al., 2020] conducted a COVID-19 modelling study, comparing R_0 for North Carolina, USA to that of the Charlotte Metropolitan Region within North Carolina. They found that R_0 was lower for the central urban area than it was for the state as a whole. Moreover, those living in rural regions are currently facing inequities in access to COVID-19 vaccines. While the Pfizer vaccine is currently the most predominant source of Canada's COVID-19 vaccine [Government of Canada, 2021b], it must be kept at temperatures between -60 to -80 degrees Celsius before administering vaccine injections [Centres for Disease Control and Prevention, 2021]. This requires specialized freezers and is less readily available in remote regions, as indicated by the fact that Canada's northern territories - Yukon, Northwest Territories, and Nunavut - have not currently been delivered the Pfizer vaccine [Government of Canada, 2021b]. Thus, the non-medical interventions will likely still be relevant during the current vaccination phase, further providing justifications for regional modelling for COVID-19 transmission.

Mathematical modelling is an indispensable part of infectious disease epidemic/pandemic response plans. These models inform policymakers regarding how infectious diseases would behave and, thus, allow measures to be put in place to help mitigate and prevent the spread of

disease [Overton et al., 2020]. Compartmental epidemiological models [Hethcote, 2000], such as susceptible-infectious-recovered (SIR) or susceptible-exposed-infectious-recovered (SEIR) models, are essential for modelling and making predictions about the spread of infectious diseases. As individuals within a population move through the various compartments in these models (susceptible, exposed, infectious, and recovered), key characteristics can be observed, such as estimates on the duration of epidemics, epidemiological parameters, and prediction on modelled prevalence. Recently, these compartmental models have been used to gain insight into the COVID-19 pandemic in many countries around the world [Lin et al., 2020, Youssef et al., 2020, Grave et al., 2021].

In BC, a compartmental mathematical modelling study by [Anderson et al., 2020] played an instrumental role at informing the provincial government on devising reopening plans after it shut down all but essential services on March 17, 2020. Their model assessed the spread of COVID-19 in BC and provided projections based on various levels of physical distancing. Their model was a modified SEIR model which contained the following compartments: susceptible (S); exposed (E_1); exposed, symptomatic, and infectious (E_2); quarantined (Q); and recovered or deceased (R) [Anderson et al., 2020]. Furthermore, this model differs from typical SIR/SEIR models in that each compartment in the model was replicated such that there were a series of two parallel compartments for those who did and did not engage in physical distancing. Moreover, this model contained a secondary exposed category and one for those who were in quarantine. While this model was vital in BC's response to COVID-19 at the beginning of the pandemic, it did not account for the inherent and aforementioned differences between urban and rural regions. Furthermore, there were parameters included in this model that were derived from urban data sources.

In this work, we expand on the compartmental model introduced by [Anderson et al., 2020] to account for the differences in rural and urban regions. Specifically, we propose a hierarchical Bayesian epidemiological model for COVID-19 for each of BC's five regional health authorities: Vancouver Coastal Health, Fraser Health, Interior Health, Island Health, and Northern Health. In this paper, we will refer the five regional health authorities respectively as Coastal, Fraser, Interior, Island and Northern and often refer them as regions. The former two regions contain the most populated urban areas in BC, including Greater Vancouver and the Fraser Valley, whereas the latter three regions are primarily rural and less populated. Since previous research has highlighted the inverse relationship between rurality and the likelihood of modified behaviours in response to the pandemic, model parameters such as the effectiveness of physical distancing and the effectiveness of COVID-19 testing will be regionalized to these five regions of BC. Other parameters, such as the basic reproduction number inherent to COVID-19, are common to all the regions, thus providing a hierarchical model structure. The purpose of these models is to assess the effectiveness of regional distancing measures within each region and compare these results with the predictions of a provincial-wide model, scaled by the relative proportion of population in each region. Despite the current COVID-19 immunization phase, this research is important and still relevant as BC continues to rely on non-medical interventions, such as physical distancing, to slow the spread of the virus until the province reaches herd immunity.

This paper is organized as follows. In Section 2, we describe an extension to the Bayesian epidemiological model introduced by [Anderson et al., 2020]. Specifically, in Section 2.1 and 2.2, we introduce a hierarchical Bayesian model for the five regional Health Authorities of British Columbia and discuss their regional time-varying specific parameters, such as regional relative contact reduction due to physical distancing and regional proportion of anticipated cases due to improvement in testing. In Section 3, we present our results and compare the differences in prevalence and parameters between the provincial-wide and regional specific models. Finally, we summarize our work and discuss limitations of our regional model, along with future work.

2 Modelling

In this section, we introduce an extension of the mathematical and statistical framework presented in [Anderson et al., 2020] for modelling the spread of COVID-19 throughout BC, Canada. We choose to build upon this model as it captures many of the key features required for modelling COVID-19. For example, the epidemiological model contains COVID-19 specific compartments, such as, exposed but not infectious, infectious but not symptomatic, and quarantining. In addition to these compartments, individuals practising physical distancing are accounted for, with reductions in exposure being time-dependant based on government lockdown protocols. The model also accounts for changes in test availability by allowing the proportion of infected individuals being tested to change over time while also accounting for potential delays between the onset of symptoms and getting a positive test. The resulting epidemiological model is then utilized within the statistical framework to compute the likely values of the unknown model parameters. As in [Anderson et al., 2020], we take a Bayesian approach to parameter estimation and sample values of parameters from their posterior distribution via Hamiltonian Monte Carlo (HMC). Computations are carried out in R, with use of the Stan package [Carpenter et al., 2017]. Further details regarding the statistical approach are discussed in Section 2.2.

Before we proceed to the model specifics, we highlight our proposed extensions to the model presented in [Anderson et al., 2020]. First and foremost, we regionalize the model to describe the spread of COVID-19 in each of the five major health regions of BC: Coastal, Fraser, Interior, Island, and Northern. This entails having a distinct set of differential equations in each of these regions, with certain parameters being region-specific and others shared provincial-wide. We also extend the modelling period to the end of December 2020, therefore we have included seven different physical distancing periods, based on government protocol, and four different testing periods accounting for improved test availability.

We have restricted our modelling period from March to December 2020 for two main reasons. Beginning in January 2021, BC began rolling out vaccines [Migdal A., 2020]. Accounting for this would require alterations to the epidemiological model, while this extension is well studied in the literature, this is not the main goal of this work. In addition to vaccinations, COVID-19 variants began spreading throughout BC and the rest of Canada starting in mid-December of 2020 [Martins N., 2021]. Moreover, certain variants are known to be far more infectious [BC Centre for Disease Control, 2021a], and therefore, significant changes to the modelling framework would be required to study their impact. Given that our main objective is to study the impacts of regional versus provincial-wide modelling, we have focused our attention on data between March 2020 and December 2020.

2.1 Epidemiological Model

We now present a regionalized version of the epidemiological model of [Anderson et al., 2020]. This is an SEIQR type model, meaning we include individuals in health region i which are susceptible (S^i), exposed but not infectious (E_1^i), exposed and infectious but not symptomatic (E_2^i), infected (I^i), quarantined (Q^i) and recovered (R^i). Due to the relatively small death rate for COVID-19, deaths are not accounted for in this model. In additions to these compartments, a secondary set of equations S_d^i, E_{1d}^i, E_{2d}^i, I_d^i, Q_d^i and R_d^i, is included for individuals in health region i practising physical distancing. The strictness of the physical distancing measures will vary in time due to policy changes throughout the different lockdown phases between March 1, 2020 and December 31, 2020.

Within the i^{th} health region with population N^i, the epidemiological model for individuals

not practising physical distancing is given by the following equations:

$$\begin{aligned}
\frac{dS^i}{dt} &= -\beta\left(I^i + E_2^i + f^i(t)(I_d^i + E_{2d}^i)\right)\frac{S^i}{N^i} - u_d S^i + u_r S_d^i \\
\frac{dE_1^i}{dt} &= \beta\left(I^i + E_2^i + f^i(t)(I_d^i + E_{2d}^i)\right)\frac{S^i}{N^i} - k_1 E_1^i - u_d E_1^i + u_r E_{1d}^i \\
\frac{dE_2^i}{dt} &= k_1 E_1^i - k_2 E_2^i - u_d E_2^i + u_r E_{2d}^i \\
\frac{dI^i}{dt} &= k_2 E_2^i - qI^i - \frac{1}{D} I^i - u_d I^i + u_r I_d^i \\
\frac{dQ^i}{dt} &= qI^i - \frac{1}{D} Q^i - u_d Q^i + u_r Q_d^i \\
\frac{dR^i}{dt} &= \frac{1}{D}(I^i + Q^i) - u_d R^i + u_r R_d^i.
\end{aligned} \tag{1}$$

The vast majority of the parameters in this model are taken constant throughout the province as they are inherent to COVID-19. For example, the parameter β captures the rate of transmission from the infectious to the susceptible individuals. One may argue that this should be region specific, since regions with higher population density will tend to have higher rates of transmission. Instead we take $f^i(t)$ to be region specific, where $f^i(t)$ accounts for the relative reduction in contacts for individuals practising physical distancing. We take $f^i(t)$ to be a continuous piecewise constant function, taking constant values in $(0, 1)$ during different phases of lockdown, with smaller values of f^i resulting in reduced transmission from physically distanced individuals. The parameters k_1, k_2 and $\frac{1}{D}$ quantify the progression of individuals through the compartments from E_1^i through E_2^i to R^i, whereas q captures the rate at which infected individuals begin quarantining. The parameter u_d represents the rate at which individuals switch their behaviour to begin physical distancing and u_r represents the rate at which they return to normal behaviour. We choose to take k_1, k_2, D, q, u_r, and u_d to be fixed throughout the province. As shown below, u_r and u_d also describe the asymptotic proportion of population who are practising physical distancing. Therefore, if this model is being applied in a variety of regions with drastically different perspectives on the value of physical distancing, then we would additionally suggest taking u_r and u_d to be region specific. It is important to note that this model accounts for infected individuals who do not quarantine, for example asymptomatic individuals, which may be contributing greatly to the proliferation of the disease.

Within the i^{th} health region, individuals practising physical distancing have their own set of differential equations, given by:

$$\begin{aligned}
\frac{dS_d^i}{dt} &= -f^i(t)\beta\left(I^i + E_2^i + f^i(t)(I_d^i + E_{2d}^i)\right)\frac{S_d^i}{N^i} + u_d S^i - u_r S_d^i \\
\frac{dE_{1d}^i}{dt} &= f^i(t)\beta\left(I^i + E_2^i + f^i(t)(I_d^i + E_{2d}^i)\right)\frac{S_d^i}{N^i} - k_1 E_{1d}^i + u_d E_1^i - u_r E_{1d}^i \\
\frac{dE_{2d}^i}{dt} &= k_1 E_{1d}^i - k_2 E_{2d}^i + u_d E_2^i - u_r E_{2d}^i \\
\frac{dI_d^i}{dt} &= k_2 E_{2d}^i - qI_d^i - \frac{1}{D} I_d^i + u_d I^i - u_r I_d^i \\
\frac{dQ_d^i}{dt} &= qI_d^i - \frac{1}{D} Q_d^i + u_d Q^i - u_r Q_d^i \\
\frac{dR_d^i}{dt} &= \frac{1}{D}(I_d^i + Q_d^i) + u_d R^i - u_r R_d^i.
\end{aligned} \tag{2}$$

The equations for the physical distancing individuals mirrors (1) almost exactly, with the modification that susceptible individuals have a reduced rate of infection, as seen by the additional factor of $f^i(t)$. As discussed above, $f^i(t)$ is taken to be constant during each phase of lockdown and between other key dates throughout the year, with one week transitions taken as a linear interpolant between each constant value. This results in,

$$f^i(t) = \begin{cases} 1, & t < t_1^F, \\ f_2^i + \frac{t_2^S - t}{t_2^S - t_1^F}\left(1 - f_2^i\right), & t_1^F \le t < t_2^S, \\ f_2^i, & t_2^S \le t < t_2^F, \\ f_3^i + \frac{t_3^S - t}{t_3^S - t_2^F}\left(f_2^i - f_3^i\right), & t_2^F \le t < t_3^S, \\ f_3^i, & t_3^S \le t < t_3^F, \\ f_4^i + \frac{t_4^S - t}{t_4^S - t_3^F}\left(f_3^i - f_4^i\right), & t_3^F \le t < t_4^S, \\ f_4^i, & t_4^S \le t < t_4^F, \\ f_5^i + \frac{t_5^S - t}{t_5^S - t_4^F}\left(f_4^i - f_5^i\right), & t_4^F \le t < t_5^S, \\ f_5^i, & t_5^S \le t < t_5^F, \\ f_6^i + \frac{t_6^S - t}{t_6^S - t_5^F}\left(f_5^i - f_6^i\right), & t_5^F \le t < t_6^S, \\ f_6^i, & t_6^S \le t < t_6^F, \\ f_7^i + \frac{t_7^S - t}{t_7^S - t_6^F}\left(f_6^i - f_7^i\right), & t_6^F \le t < t_7^S, \\ f_7^i, & t \ge t_7^S, \end{cases} \tag{3}$$

where the dates for t_j^S and t_j^F, for $j = 1, \ldots, 6$ are summarized in Table 1.

These change points reflect the various phases of lockdown within BC throughout 2020 as reported on [BC Centre for Disease Control, 2021b]. Specifically, Phase 1, Phase 2 and Phase 3A were between t_1^F and t_2^F, t_2^F and t_3^F, t_3^F and t_4^F respectively. According to our notation, Phase 3B would account of t_4^F to t_6^F, and we included an additional change point for Thanksgiving at t_5^F. Finally, Phase 3C took effect after t_6^F.

Start Date	End Date
	t_1^F = Mar. 14
t_2^S = Mar. 21	t_2^F = May 18
t_3^S = May 25	t_3^F = Jun. 23
t_4^S = Jun. 30	t_4^F = Sep. 12
t_5^S = Sep. 19	t_5^F = Oct. 12
t_6^S = Oct. 19	t_6^F = Nov. 7
t_7^S = Nov. 14	

Table 1: The change points are used in the definition of $f^i(t)$. We note that all dates (except Thanksgiving) were obtained from [BC Centre for Disease Control, 2021b].

As discussed above, u_r and u_d also determine the asymptotic proportion of the population following physical distancing protocols. This follows by defining $P^i(t) = S^i(t) + E_1^i(t) + E_2^i(t) + I^i(t) + R^i(t) + Q^i(t)$ and $P_d^i(t) = S_d^i(t) + E_{1d}^i(t) + E_{2d}^i(t) + I_d^i(t) + R_d^i(t) + Q_d^i(t)$, to represent the non-physically distanced population and the physically distanced population in the i^{th} health region respectively. Using the systems (1) and (2) we obtain $\frac{d}{dt}P^i(t) + \frac{d}{dt}P_d^i(t) = 0$, implying $P^i(t) + P_d^i(t) = N^i$, the total population of our modelled region. This is as expected, since we are not accounting for birth or death. Taking $P^i(t) = N^i - P_d^i(t)$, we obtain the differential equation $\frac{d}{dt}P_d^i(t) = u_d N^i - (u_r + u_d)P^i(t)$, which implies that $P_d(t) = \frac{u_d}{u_r + u_d}N^i$ is a globally asymptotically stable fixed point of $\frac{d}{dt}P_d^i(t)$. Therefore, the system of differential equations

in health region i, (1) and (2), rapidly converges to $\frac{u_d}{u_r+u_d}N^i$ individuals practising physical distancing.

Throughout this paper we will distinguish between the basic reproduction number inherent to the disease, denoted R_{0b}, and the regionalized basic reproduction number, denoted R_0^i, where factors such as physical distancing and quarantining are taken into account. We obtain R_{0b} by computing the basic reproduction number of a simplified version of (1), without physical distancing or quarantining. This can be done, for example, using the next-generation method [Diekmann et al., 1990, van den Driessche and Watmough, 2002], where E_1^i, E_2^i, and I^i are taken as the disease states. This yields $R_{0b} = \frac{\beta}{D+1/k2}$ which is constant throughout the province since β, D, and k_2 are not regionalized constants. As shown in Appendix A of [Anderson et al., 2020], the next-generation method can also be used to compute the regionalized basic reproduction number R_0^i, given by

$$\begin{aligned} R_0^i(t) = \beta\Bigg(& \frac{e^4(1-e)(1-f^i(t))^2k_1k_2}{(e(\frac{1}{D}+q)+1)(ek_1+1)(ek_2+1)} + \frac{(ef^i(t)+1-e)^2}{\frac{1}{D}+q} \\ & + \frac{ek_1(ef^i(t)+1-e)^2}{k_2(ek_1+1)(ek_2+1)} + \frac{e(ef^i(t)+1-e)^2}{(ek_1+1)(ek_2+1)} \\ & + \frac{(ef^i(t)+1-e)^2}{k_2(ek_1+1)(ek_2+1)} + \frac{e^2k_1(e(f^i(t))^2+1-e)}{(ek_1+1)(ek_2+1)}\Bigg), \end{aligned} \tag{4}$$

where e represents the asymptotic proportion of individuals practising physical distancing, given by $e = \frac{u_d}{u_r+u_d}$.

Given that $R_0^i(t)$ depends on $f^i(t)$, it therefore varies in time as $f^i(t)$ transitions from t_j^F to t_{j+1}^S, $j = 1, \dots 6$, and varies based on the region i. With the epidemiological model established, we now shift our focus to the statistical aspects of our model.

2.2 Statistical Modelling

The ordinary differential equations (1) and (2) are solved within Stan using a numerical ODE solver that includes arguments: t (independent variable time), state (the ODE system at the time specified), θ (the ODE arguments that depend on parameters), x_r (the ODE arguments that depend on data only) and x_i (the integral data values used to evaluate the ODE system).

To relate the flow of individuals from the compartments of (1) and (2) to testing data, we define the expected number of reported cases on day r to be μ_r, given by

$$\mu_r^i = \psi^i(r) \int_0^{45} k_2 \left[E_2^i(r-s) + E_{2\mathrm{d}}^i(r-s)\right] w(s)\mathrm{d}s, \tag{5}$$

where $\psi^i(r)$ is the proportion of anticipated cases in the i^{th} health region on day r that are tested and reported, and $w(s)$ is the density function of delay s, with a maximum delay of 45 days, where $w(\cdot)$ denotes the Weibull distribution. The histogram of times between symptoms onset and case reporting was fitted using Weibull distribution [Anderson et al., 2020], in which the 99.99992% quantile of 45 days is set to be the maximum delay.

Furthermore, given that testing protocol and availability evolved throughout the pandemic, we define $\psi^i(r)$ to be the piecewise function

$$\psi^i(r) = \begin{cases} \psi_1^i, & \text{March 1} \le r \le \text{March 15}, \\ \psi_2^i, & \text{March 16} \le r \le \text{April 8}, \\ \psi_3^i, & \text{April 9} \le r \le \text{April 20}, \\ \psi_4^i, & \text{April 21} \le r \le \text{December 31}, \end{cases} \tag{6}$$

We chose these change points for $\psi^i(r)$ because starting on March 16, 2020, the testing shifted focus to healthcare workers, long-term care residents, and community clusters not linked to travel. Then from April 9, 2020, expanded testing included residents in remote regions, people in homeless or unstable housing, first responders and returning travellers to Canada. Finally from April 21 and onwards, any individual with COVID-19 symptoms was eligible to get a test.

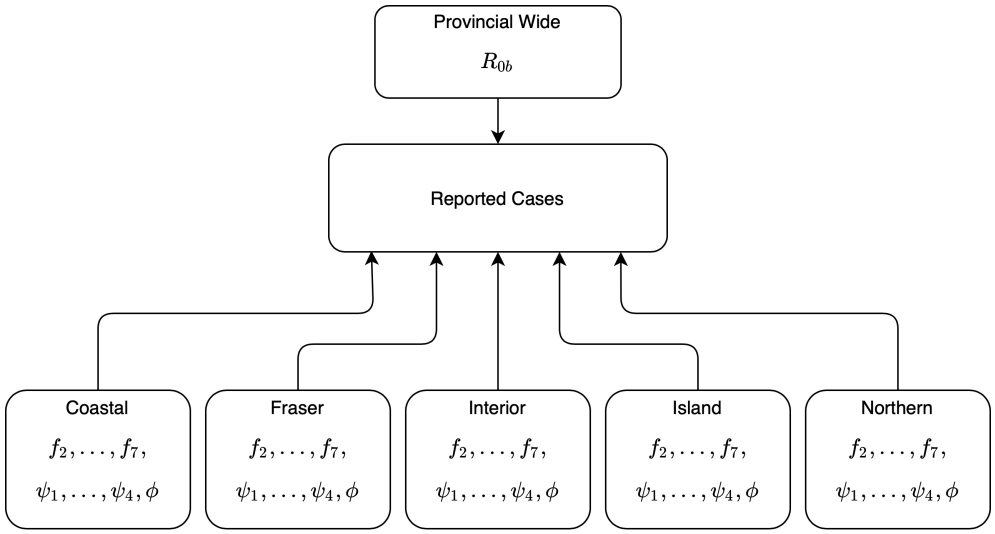

Figure 1: This depicts the hierarchical structure of the model dependence on parameters. R_{0b} is shared between all regions and $f_2, \ldots, f_7$, $\psi_2, \ldots, \psi_4$ and ϕ are individualized to each region.

There are certain disadvantages in having purely regional models. For example, for a small region like Northern, the number of cases being sampled is very low. Since we have a small sample size, there is a lot more variability, which may lead to unreliable estimates. To deal with this problem, we used hierarchical modelling to have all five regions share the same R_{0b} with the prior Lognormal $(\log(2.6), 0.2)$, as illustrated in Figure 1. This combines regional and information from throughout BC to help smooth out the estimates, meaning the estimates are not purely driven by local dynamics. As discussed in Section 2.1, R_{0b} represents the basic reproduction number inherent to COVID-19, thus we model R_{0b} to be constant across all regions. The rate of spread within each region is then determined through the regional specific parameters $f_2^i, \ldots, f_7^i$. For various values of R_{0b}, we expect the epidemiological model (1) to alter its prediction, with larger R_{0b} resulting in an increased number of predicted cases. This is indeed the case, since $R_{0b} = \frac{\beta}{(D+1/k2)}$. As discussed in Section 2.3, the parameters D and k_2 are fixed, therefore we ensure that the dynamics of (1) reflect a given value of R_{0b} by setting $\beta = R_{0b}(D + 1/k2)$.

For each region in the hierarchical model, we used a negative binomial observation model to link the expected case count in region i, μ_r^i from the structural model, and the observed case count data in region i, denoted by C_r^i:

$$NB2\left(C_r^i \mid \mu_r^i, \phi^i\right) = \left(\begin{array}{c} C_r^i + \phi^i - 1 \\ C_r^i \end{array}\right)\left(\begin{array}{c} \mu_r^i \\ \mu_r^i + \phi^i \end{array}\right)\left(\begin{array}{c} \phi^i \\ \mu_r^i + \phi^i \end{array}\right)^{\phi^i}$$

where ϕ^i is the (inverse) dispersion parameter with prior $1/\sqrt{\phi^i} \sim Normal(0, 1)$.

Taking a Bayesian approach, the corresponding statistical model has parameters R_{0b}, f_k^i, ψ_j^i and ϕ^i, for $k = 2, \ldots, 7$ and $j = 1, \ldots, 4$, and the joint posterior distribution of the parameters

can be written as

$$[R_{0b}, \boldsymbol{f}_2, \ldots, \boldsymbol{f}_7, \boldsymbol{\psi}_1, \ldots, \boldsymbol{\psi}_4, \boldsymbol{\phi} \mid \boldsymbol{C}] \propto$$
$$[R_{0b}] \prod_{i=1}^{5} \left\{ \left[\boldsymbol{C}^i \mid R_{0b}, f_2^i, \ldots, f_7^i, \psi_1^i, \ldots, \psi_4^i, \phi^i\right] \left[f_2^i\right] \ldots \left[f_7^i\right] \left[\psi_1^i\right] \ldots \left[\psi_4^i\right] \left[\phi^i\right] \right\}, \tag{7}$$

where $\left[\boldsymbol{C}^i \mid R_{0b}, f_2^i, \ldots, f_7^i, \psi_1^i, \ldots, \psi_4^i, \phi^i\right]$ represents the negative binomial data likelihood for region i, the prior distributions are shown by $[R_{0b}], [f_2^i], \ldots, [f_7^i], [\psi_1^i], \ldots, [\psi_4^i]$ and $[\phi^i]$, and $\boldsymbol{C}^i$ is the vector of reported cases for each region. The prior distributions of $[R_{0b}], [f_2^i], \ldots, [f_7^i]$, and $[\psi_1^i], \ldots, [\psi_4^i]$ are summarized in Table 2. The priors chosen for $f_2^i \ldots f_7^i$ reflect the gradual loosening of restriction between March 21, 2020 and November 6, 2020, and tightening of restrictions starting from November 7, 2020. In general, these priors encode our knowledge of policy and testing protocols, while being flexible enough (via prior standard deviations of 0.2 for $f_2^i \ldots f_7^i$ and 0.05 for $\psi_1^i, \ldots, \psi_4^i$) to allow the data to inform the final parameter estimates.

Parameter	Prior Distribution	Mean	Standard Deviation
R_{0b}	Lognormal $(\log(2.6), 0.2)$	2.6525	0.2871
f_2^i	Beta$(2, 3)$	0.4	0.2
f_3^i	Beta$(2.625, 2.625)$	0.5	0.2
f_4^i	Beta$(3, 2)$	0.6	0.2
f_5^i	Beta$(2.975, 1.275)$	0.7	0.2
f_6^i	Beta$(2.4, 0.6)$	0.8	0.2
f_7^i	Beta$(3, 2)$	0.6	0.2
ψ_1^i	Beta$(3.5, 31.5)$	0.1	0.05
ψ_2^i	Beta$(12.6, 50.4)$	0.2	0.05
ψ_3^i	Beta$(24.9, 58.1)$	0.3	0.05
ψ_4^i	Beta$(38, 57)$	0.4	0.05

Table 2: The prior distributions for the parameters in the statistical model

2.3 Provincial and Regional Model Inputs

Table 3 shows the populations of each region [Interior Health, 2020]. This was used for initialization and comparison with the provincial-wide model. Moreover, we have used the value of N =5,100,000 in our provincial-wide model for the population of BC[1].

Region	Population
Coastal	1,225,195
Fraser	1,889,225
Interior	795,116
Island	843,375
Northern	297,570

Table 3: Populations of each regional Health Authority in BC.

For a given set of parameters $f_1^i, \ldots, f_7^i$ and R_{0b}, or equivalently β, we need to solve the equations (1) and (2) in each region. To do this we need appropriate initial conditions for

[1]Although the sum of the regional population is 5050481, we have used the same provincial-wide population as [Anderson et al., 2020] for consistency.

the differential equations, requiring initial values for all model compartments in all five regions. These values were obtained for the provincial-wide model, as discussed in [Anderson et al.,2020], by initializing the model on February 1 with 8 individuals shared between compartments E_1, E_2, I and E_{1d}, E_{2d} and I_d. The specific initial conditions among these compartments is displayed on Table 2 of [Anderson et al.,2020]. Using these initial conditions, equations (1) and (2) are solved throughout February using $\psi(r)$ between 10% and 30%, and without incorporating any additional data. The resulting distribution of values throughout the compartments on March 1 was then taken as the initial condition for computations starting on March 1. We follow this same methodology to obtain initial values in each of the five regions by scaling down provincial-wide compartmental values on March 1 based on the relative population. For example, $S^i(\text{March 1}) = \frac{N^i}{N} S(\text{March 1})$, where S denotes total number of susceptible individuals provincial-wide and N is the total population of BC.

As discussed in Section 2.1, the parameters k_1, k_2, u_r, u_d, q and D are taken to be constant across all five regions. Although u_r and u_d were discussed in detail within Section 2.1, it remains to justify this choice for the other parameters. Note that k_1 and k_2 describe the rates of transition from E_1^i to E_2^i and E_2^i to I^i respectively. This rate is inherent to the virus as it describes the evolution of the disease, for example, k_1 represents the rate of transition from exposed and not infectious to exposed and infectious but not symptomatic. Similarly, parameter D represents the mean duration of the infectious period (the average time spent in compartment I^i in the absence of quarantining). Parameter q however, represents the rate at which infectious individuals begin fully quarantining. As discussed in [Anderson et al., 2020], it was estimated early in the pandemic that one fifth of all severe cases eliminated transmission by rather fully quarantining, or ending up in the hospital (both of these outcomes are considered to be within compartment Q^i). Referencing equation (1), individuals can leave compartment I^i and remain in the non-distanced group, by staying in I for the full duration D then entering compartment R^i, or by beginning to quarantine at rate q. Therefore, the proportion of individuals exiting I^i to quarantine versus staying in I for the full duration is given by $\frac{q}{q+1/D}$. Equating this ratio to $1/5$ and setting $D = 5$ yields our choice of $q = 0.05$. One may argue that this value may have changed throughout the year or may be regionally dependent. However, allowing this to vary would directly impact the resulting values of $f^i(t)$, therefore, to accommodate any changes that may occur throughout the year or regionally, we let the physical distancing parameter $f^i(t)$ vary to compensate. The remaining values for these parameters are as follows: $k_1 = 0.2$ days^{-1}, $k_2 = 1$ days^{-1}, see [Tindale et al., 2020, Ganyani et al., 2020], and $(u_d, u_r) = (0.1, 0.02)$, see [Korzinski D. and Kurl S., 2020].

The data used in this research is publicly available from the British Columbia Centre for Disease Control website [BC Centre for Disease Control, 2021b]. At the time that this project commenced, the data for all health authorities was downloaded in a single CSV file and were manually organized by region. During the time frame under investigation in this work, BC experienced two waves of COVID-19 cases. The first occurred from March to early April of 2020, where the seven-day moving average of cases reached approximately 50 cases per day. From the beginning of April onward, case numbers were very low and remained that way until they started climbing at the beginning of July 2020. The second wave surge commenced at the end of October 2020. The seven-day moving average of cases skyrocketed from 150 cases per day to just under 800 cases per day by the beginning of December 2020 before tapering off and plateauing at approximately 500 cases per day for the remainder of 2020.

3 Results and Discussion

In this section, we present numerical results which highlight the differences between provincial and regional modelling. We focus on two comparisons, the first being a full analysis using reported cases from March 1 to December 31, comparing the prevalence between the provincial-wide and regional models. The second comparison is a predictive test, where we use the data from March 1 to November 7 and let both models predict the future prevalence. Overall both comparisons show significant differences between the regional and provincial-wide models. Below, we present a detailed discussion of these results and the associated figures. To obtain the numerical results, we used Stan 2.21.0 and R 4.0.2, running 2000 HMC iterations and 4 chains for all our runs. All 4 chains were observed to have converged as shown in the trace plots of Figures 8-11 from Appendix A.

Before analyzing the results, we clarify how we compute the provincial-wide model and compare its results with the regional model. For the provincial-wide model, we have a single set of differential equations (1) and (2), with the same initial conditions in [Anderson et al., 2020]. To ensure a fair comparison between the regional and provincial-wide models, we impose the same model structure on the provincial-wide model. Specifically, we introduce the same change points for $f_2, \ldots, f_7$ and $\psi_1, \ldots, \psi_4$, with the same priors on all model parameters. Finally we take N to be the entire population of the province. To compare with regional specific results, we have scaled our provincial-wide results using the regional population ratios, with Coastal by 0.24, Fraser by 0.37, Interior by 0.16, Island by 0.17 and Northern by 0.06.

3.1 Comparison between Provincial-wide and Regional Models

In this section, we compare the results between the regional and provincial-wide models, using data from March 1 to December 31. In particular, our objective is to compare the differences in COVID-19 prevalence arising between the regional and provincial-wide models. Recall that by prevalence, we refer to the total number of COVID-19 cases, not just the cases accounted for via testing. Figure 2 displays the estimated densities for R_{0b} of the hierarchical regional model in blue and the provincial-wide model in red. The difference between these densities is negligible, with the means being 3.07 and 3.06 for the hierarchical regional model and the provincial-wide model respectively.

The plots in Figure 3 showcase the differences between the regional $f_2^i, \ldots, f_7^i$ and the provincial-wide $f_2, \ldots, f_7$, where we recall that f_j^i represents the fraction of normal contacts in region i during phase j. Our first observation is that within the more populous Fraser and Coastal regions, the differences in regional and provincial-wide f_i are minimal. Alternatively, there is significant variation between the regional and provincial-wide f_i in the Island, Interior and Northern regions. Moreover, we can study each region to compare the resulting f_j^i versus f_j. For example, we see that the provincial-wide and regional models in the Northern region have similar f_2, f_3, and f_4. However, we see differing values for f_5, f_6 and f_7. These differences, as discussed below, result in wildly different prevalence. Similar observations can be made in other regions as well.

Combining the results of the hierarchical regional R_{0b} and the provincial-wide R_{0b} from Figure 2 and the mean values of the regional f_j^i and the provincial-wide f_i from Figure 3, equation (4) was used to compute Table 4. Here we see the resulting values of R_0^i along with its regional weighted average R_0 and the provincial-wide R_0. We note that there is good agreement between the regional weighted average R_0 and the provincial-wide R_0. Using these observations on the regional and provincial-wide R_0 values, we focus next on the differences in predicted prevalence between the regional and provincial-wide model.

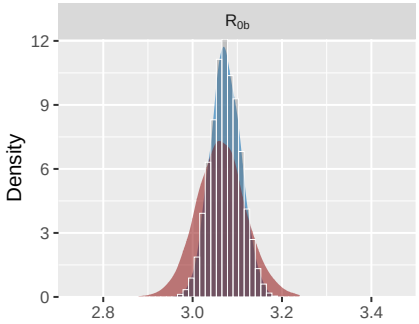

Figure 2: R_{0b} comparison of hierarchical regional model (blue) vs provincial-wide model (red).

Region	f_2	f_3	f_4	f_5	f_6	f_7
Coastal R_0	0.48	1.44	1.31	0.77	1.74	0.77
Fraser R_0	0.66	1.22	1.47	1.22	1.60	0.85
Interior R_0	0.31	2.19	0.92	1.35	1.74	1.11
Island R_0	0.22	1.64	1.17	0.82	2.35	0.78
Northern R_0	0.41	1.35	1.35	0.64	2.03	1.17
Regional Weighted Average R_0	0.48	1.51	1.29	1.03	1.81	0.88
BC wide R_0	0.56	1.25	1.22	1.05	1.67	0.87

Table 4: Listed are the values for the regionalized basic reproduction number R_0^i using mean values of f_j^i and R_{0b}, the weighted average of the R_0^i based on the regional population ratio, and the provincial-wide basic reproduction number R_0.

Figure 4 shows the discrepancies between the regional and provincial-wide model prevalence of COVID-19 between March 1 and December 31, 2020. First, we see vast differences in the prevalence in the Interior region, Island region and Northern region. Within the Island region for example, the provincial-wide model grossly overestimates the number of cases, whereas in the Interior and Northern regions the provincial-wide model predicts decline through late November and December, when in fact the prevalence in these two regions were increasing. In Figure 5, we observed that the regional model is in good agreement with the reported cases and hence we believe the regional model provides a more accurate estimate of the modelled prevalence in Figure 4. Moreover, we observed that the values of R_0^i and R_0 are consistent with the plots in Figure 4. For example, the first vertical dashed line is where f_2 begins. Referring to Table 4, we see that the R_0^i values corresponding to the f_2 column are all less than 1, meaning the prevalence should decrease, which is exactly what we observe in each region of Figure 4. Similarly for f_3 and f_4 columns of Table 4, we see that the R_0^i values are larger than 1 for the Coastal, Fraser, Island and Northern regions, which is in good agreement with their increase in prevalence during the same period. Moreover, for the R_0^i values in the f_5 column of Table 4, the R_0^i values of the Fraser and Interior region are larger than 1, while the Coastal, Island and Northern regions are less than 1. These values are in good agreement with the regional prevalence of Figure 4 in that time period. These patterns hold in the remaining regions and phases, as we see the correct correlation between rise and fall of the prevalence and the respective R_0^i being greater or smaller than 1.

Overall, the results in this section indicate that a provincial-wide model is unable to accurately capture the modelled prevalence throughout all regions. For instance, during the December period, the differences in the Island region are so significant that government regulations based on provincial-wide modelling may be overly restrictive. Alternatively, the provincial-wide model would indicate a large decline of cases in the Interior and Northern regions, potentially leading to a loosening of restrictions. However, based on the rising cases in regional modelled prevalence, loosening of restrictions would be the incorrect course of action for these regions.

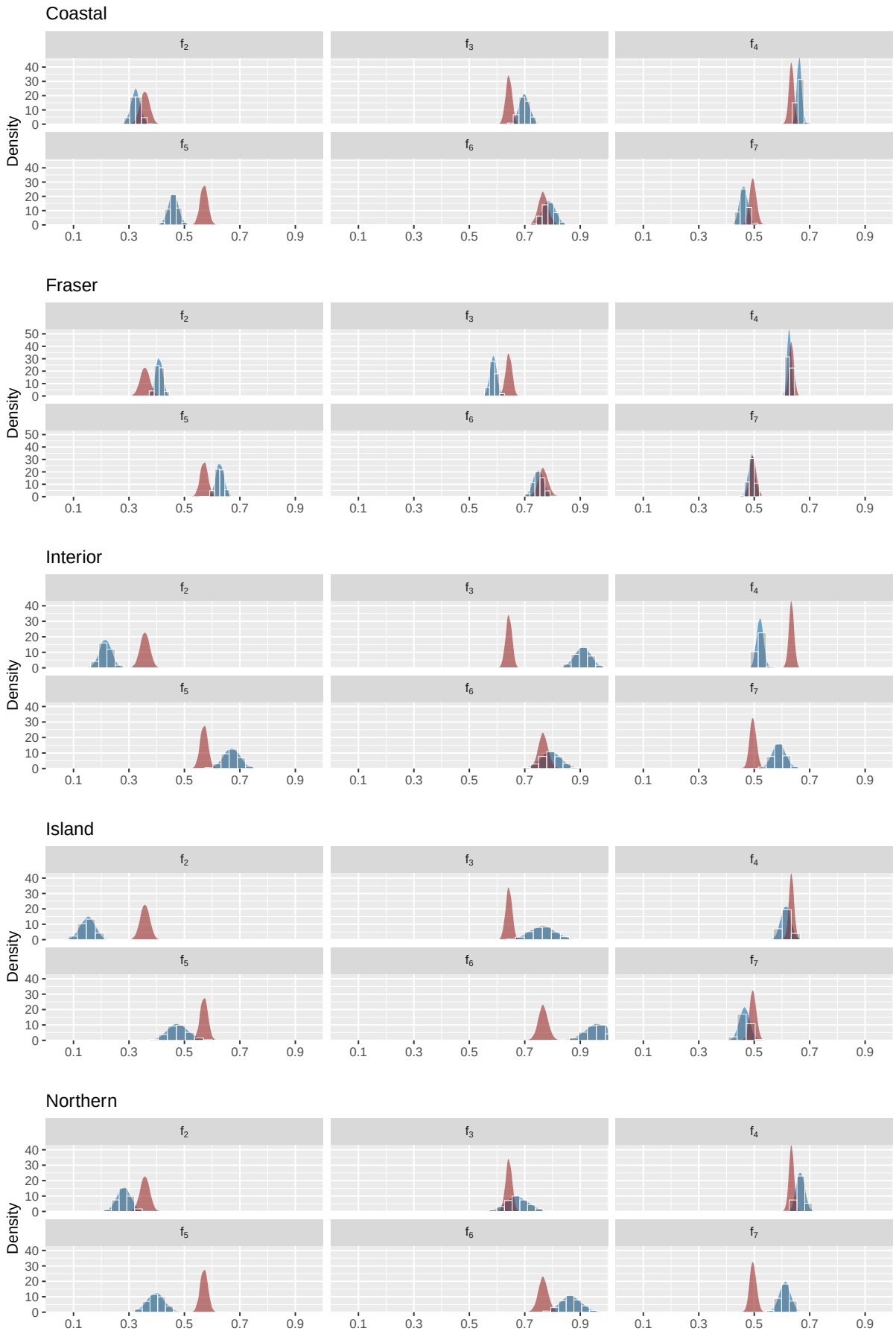

Figure 3: Comparison of estimated densities for $f_2, \ldots, f_7$ by regions (blue) and provincial-wide (red).

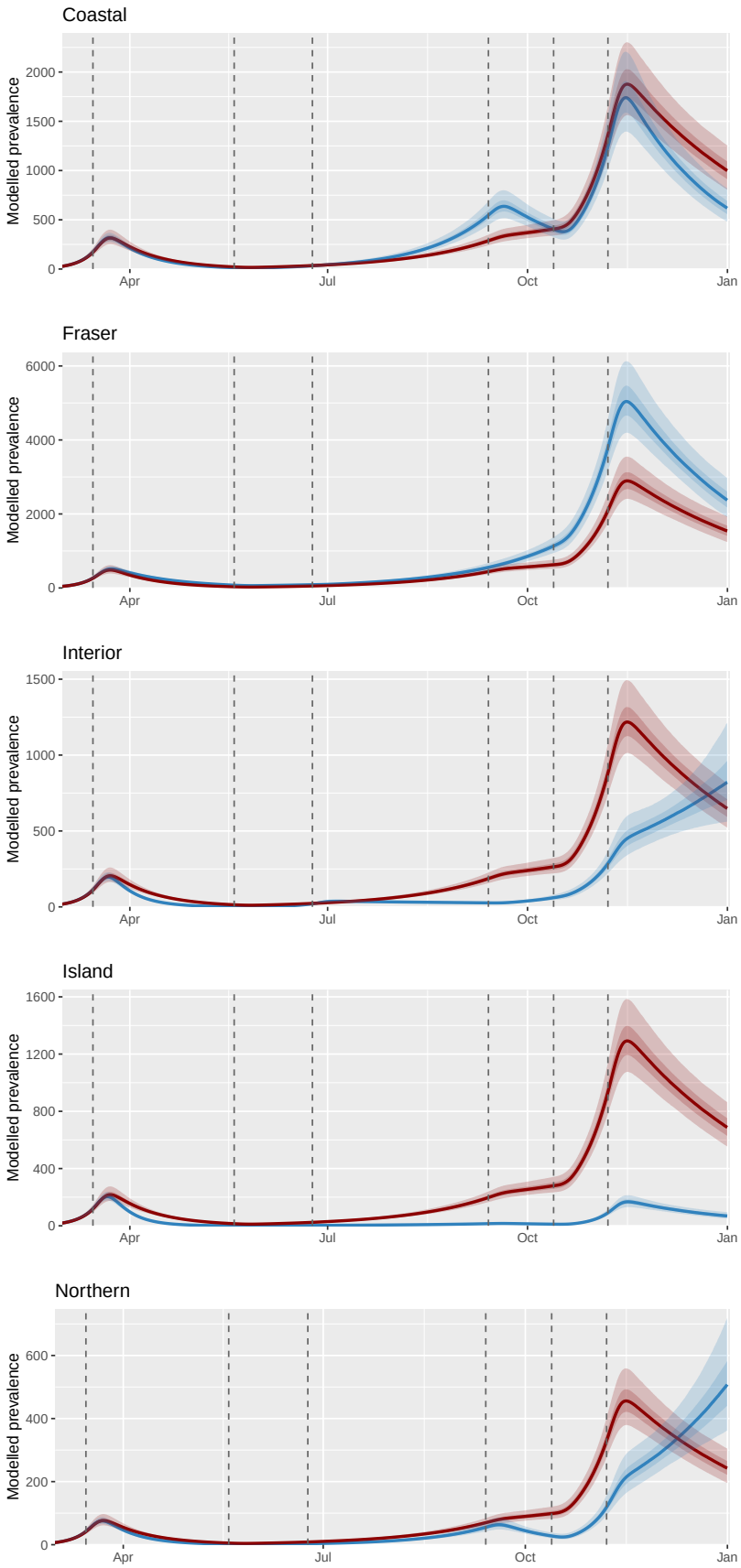

Figure 4: Comparison of modelled prevalence by regions (blue) and provincial-wide (red) scaled by respective regional population ratios. The dotted lines indicate start of reopening phases of $f_2^i, \ldots, f_7^i$, as detailed in Table 1. Here, the solid lines indicate the respective mean and shaded regions indicate respective 50% and 90% credible intervals.

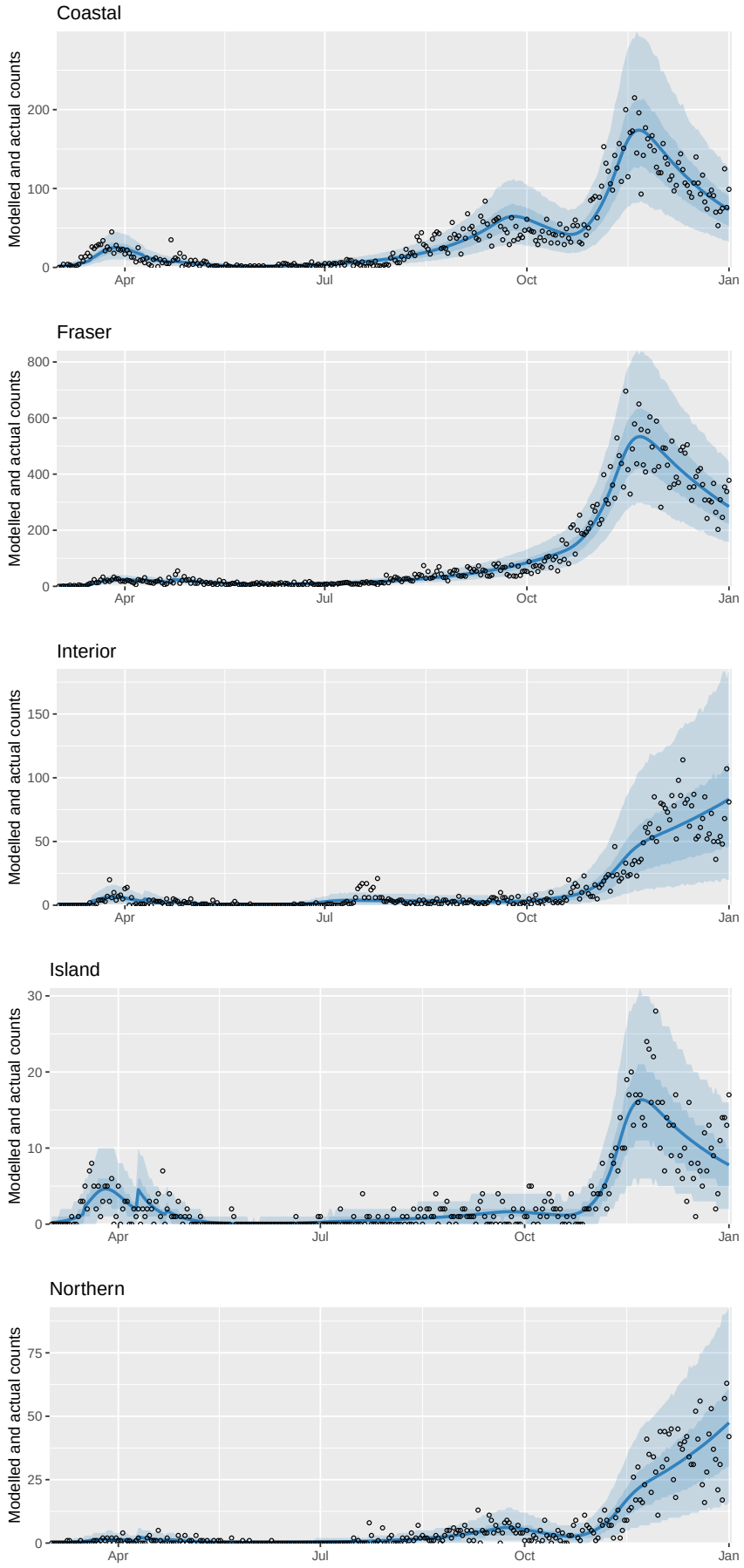

Figure 5: Comparison on reported (dots) and modelled cases (blue) of each region. Solid blue line indicate the mean and blue shaded regions indicate 50% and 90% credible intervals.

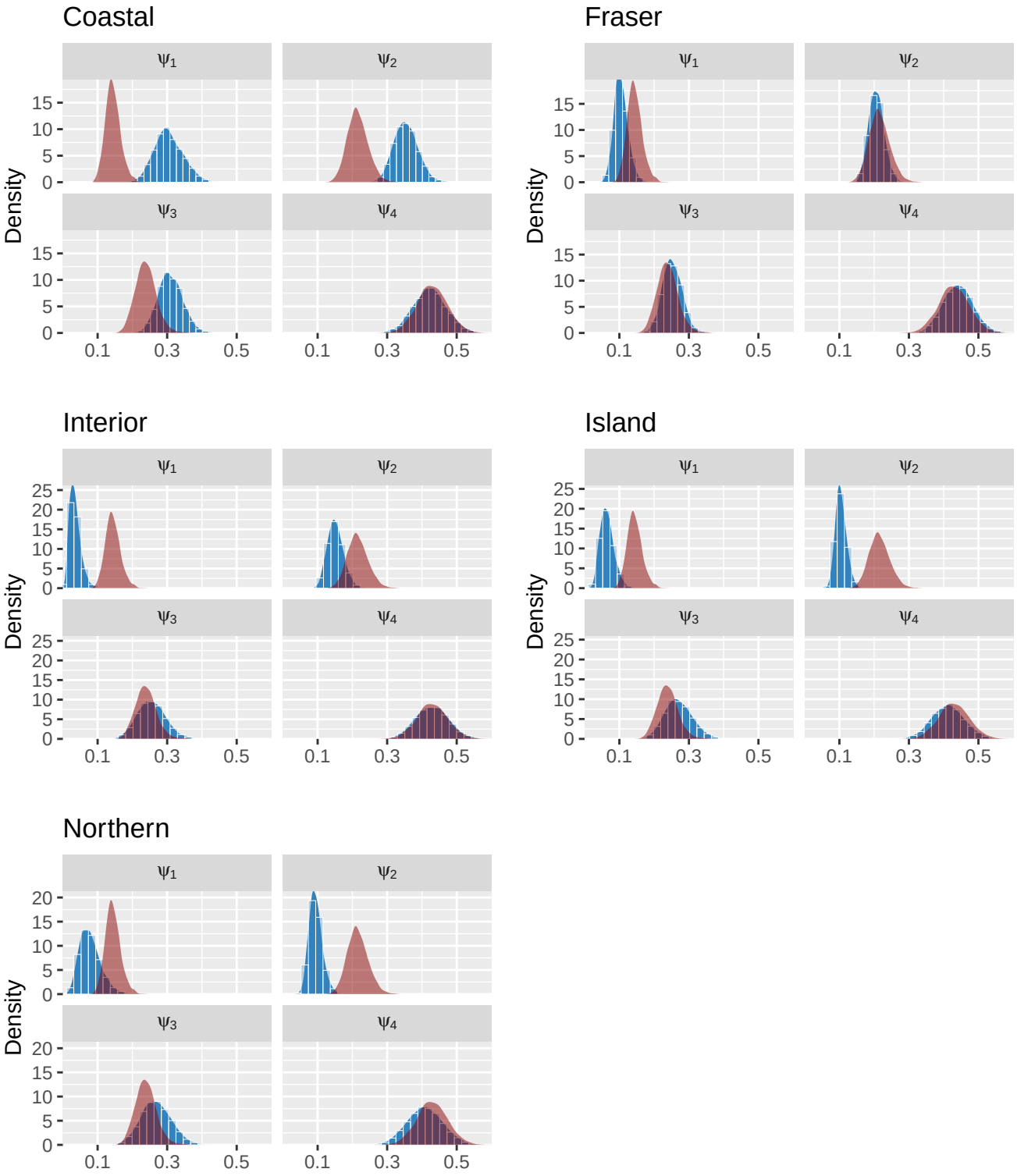

Figure 6: Comparison of estimated densities for $\psi_1, \ldots, \psi_4$ by regions (blue) and provincial-wide (red).

Finally, Figure 6 plots the estimated densities of $\psi_1, \ldots, \psi_4$, namely the proportion of anticipated cases that are tested and reported, shown in blue for each region. Again for comparison, the corresponding density estimates for these parameters in the provincial-wide model are shown in red. There are some apparent differences between the regionally and provincially estimated ψ_1 and ψ_2. As these are the early weeks of the pandemic, this indicates that there may be uneven testing availability in the province. Furthermore, there is uncertainty arising from the assumed initial conditions for the model (due to low initial case counts) that may account for

these differences. Once testing became widely available (April 21 onwards, represented by ψ_4), it appears that all the individual regions stabilize at detecting about 40% of their anticipated cases, which thus matches the overall provincial estimate.

3.2 Comparison on Prediction between Provincial-wide and Regional Models

For this comparison, we used data from March 1 to November 7, 2020 to fit the models, and subsequently predict the prevalence of COVID-19 cases in the time period between November 8 and November 31, 2020. The resulting plots are shown in Figure 7. In many ways, this set of plots is the most impactful of our presented results, as we now explain.

The epidemiological model described by (1) and (2), with parameters estimated via the statistical methodology presented in Section 2.2, yield our best estimates of how the pandemic is evolving at a given time, and quantify the uncertainty associated with those estimates (via credible intervals). We verified that these parameters allow us to fit the regional data remarkably well, as seen in Figure 7. The final step is to use this model for prediction, as shown in the light grey portions of the plots. Focusing our attention to the Interior, Island and Northern region plots of Figure 7, we see a very large overestimation of cases by the provincial-wide predictions. As discussed in the modelled prevalence in Section 3.1, this overestimation may lead to overly restrictive government lockdown. Conversely, focusing now on the Fraser region, we see that the regional model predicts slightly more cases than the provincial-wide model, indicating further restrictions may be needed to prevent overwhelming the regional health care system. Overall, these results further emphasize the importance of regionalized modelling for accurate estimation of future prevalence.

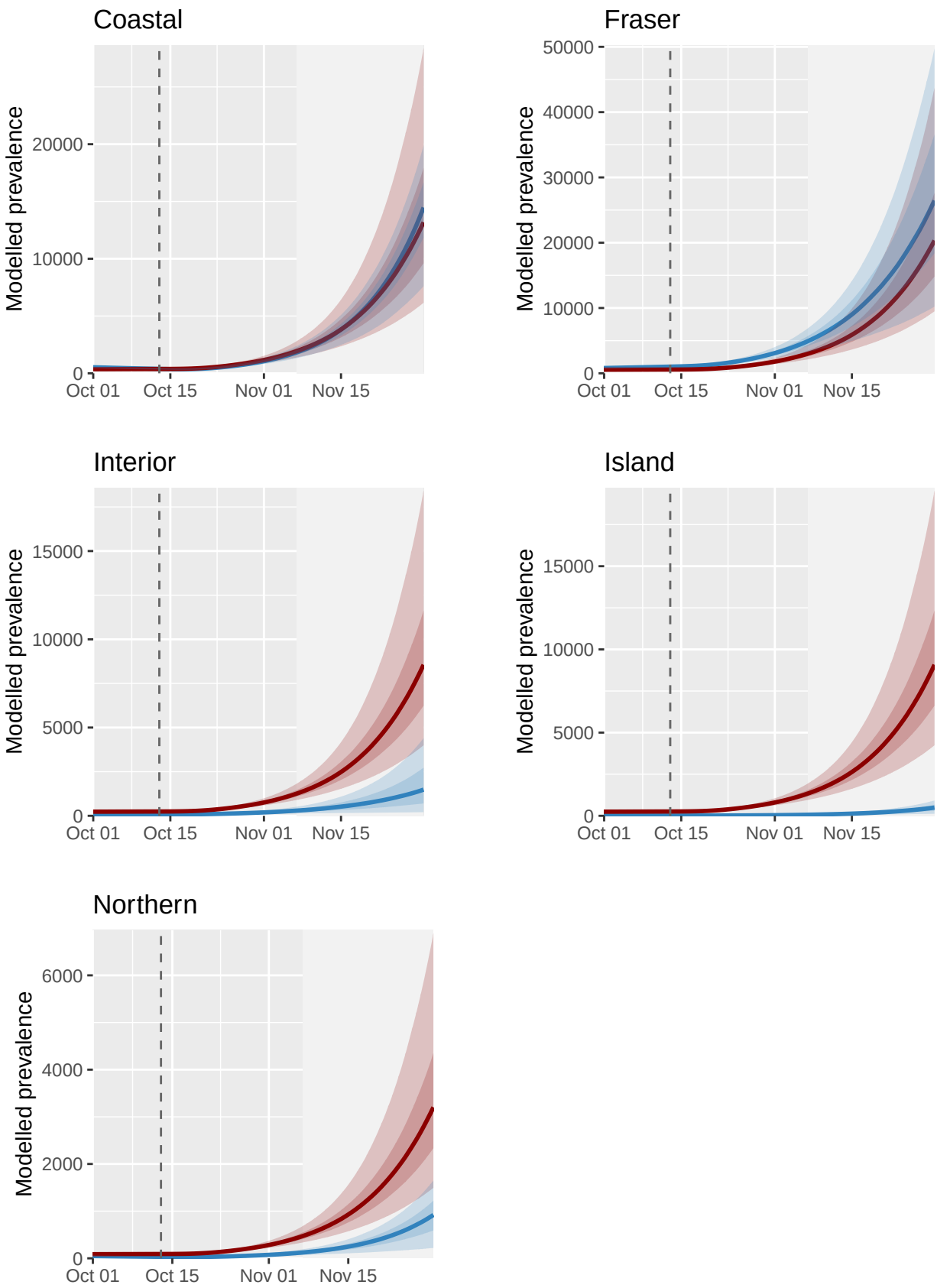

Figure 7: Comparison of predicted modelled prevalence by regions (blue) versus provincial-wide (red). Dotted line indicate start of f_6^i on October 12th and the light grey regions indicate prediction region starting from November 7th. Again, solid lines indicate the respective mean and shaded regions indicate respective 50% and 90% credible intervals.

4 Conclusion

This paper presented a hierarchical regional approach for the modelling of COVID-19 prevalence in BC, to assess the effectiveness of public health measures in reducing physical contacts in 2020. Compared to previous applications of this epidemiological compartment model, we introduced an additional hierarchical structure to facilitate regional-level modeling, with parameters specified such that some are region-specific and others are common to all regions. The results showed important differences between this regional model and the corresponding provincial-wide model, in both prevalence estimates and also for prediction. This in turn suggests that regionalized models and interventions can be crucial for addressing the future prevalence of COVID-19.

The model presented nonetheless has certain limitations. The ODE systems do not account explicitly for migration between regions; such migration could have played a key role especially during the initial spread of COVID-19 to the different regions of the province. Also, we did not attempt to incorporate time-varying or region-specific parameters u_d and u_r which govern the attitudes towards physical distancing, but rather captured their effects within the f_i parameters for simplicity. For example, u_d and u_r may have changed as the pandemic progressed due to lockdown fatigue. We also note that data on the number of tests performed and positivity rates have not been used in the model; intuitively, these may have some relationship to ψ_i but their actual role is difficult to determine, without random testing.

Furthermore, upon finishing our work, we have noticed that the BC Centre for Disease Control has started reporting regional predictions in their weekly report as of the week of April 14, 2021 [BC Centre for Disease Control, 2021c] as well as in their recent annual report [BC Centre for Disease Control, 2021d]. Thus, another extension to this work would be to modify our hierarchical Bayesian epidemiological model to incorporate vaccinated individuals and additional modifications to account for more infectious variants of COVID-19. With additional change points to account for recent restrictions in 2021, the modified model would allow predictions to be made with the current 2021 data for comparison with the regional predictions from the BC Centre for Disease Control.

Funding Acknowledgements

Samuel W.K. Wong's research was partially supported by a Discovery Grant from the Natural Sciences and Engineering Research Council (NSERC) of Canada. Jennifer Tippett was a former University of Northern British Columbia (UNBC) Masters student and her research in this work were supported by the NSERC COVID-19 Supplement. Geoffrey McGregor is a UNBC postdoctoral fellow, and his research and Andy Wan's research were partially supported by the NSERC Discovery Grant Program.

Author Information and Contribution

The authors have no competing interests declared.

Geoffrey McGregor (UNBC)
Contribution: Model Analysis, Validation, Methodology, Writing, Review and Editing

Jennifer Tippett (UNBC)
Contribution: Data curation, Writing, Review and Editing

Andy T.S. Wan (UNBC)

Contribution: Conceptualization, Validation, Methodology, Visualization, Writing, Review, Editing and Supervision

Mengxiao Wang (University of Waterloo)
Contribution: Data curation, Statistical Analysis, Visualization, Writing, Review and Editing

Samuel Wong (University of Waterloo)
Contribution: Validation, Methodology, Statistical Analysis, Visualization, Writing, Review, Editing and Supervision

References

[Anderson et al., 2020] Anderson, S. C., Edwards, A. M., Yerlanov, M., Mulberry, N., Stockdale, J. E., Iyaniwura, S. A., Falcao, R. C., Otterstatter, M. C., Irvine, M. A., Janjua, N. Z., Coombs, D., and Colijn, C. (2020). Quantifying the impact of COVID-19 control measures using a Bayesian model of physical distancing. *PLOS Computational Biology*, 16(12):1–15.

[BC Centre for Disease Control, 2021a] BC Centre for Disease Control (2021a). BC Centre for Disease Control: COVID-19 Variants. `http://www.bccdc.ca/health-info/diseases-conditions/covid-19/about-covid-19/variants`. Retrieved on April 15, 2021.

[BC Centre for Disease Control, 2021b] BC Centre for Disease Control (2021b). BC COVID-19 Data. `http://www.bccdc.ca/health-info/diseases-conditions/covid-19/data`. Retrieved on April 15, 2021.

[BC Centre for Disease Control, 2021c] BC Centre for Disease Control (2021c). British Columbia (BC) COVID-19 Situation Report Week 13: March 28–April 3, 2021. `http://www.bccdc.ca/Health-Info-Site/Documents/COVID_sitrep/Week_13_2021_BC_COVID-19_Situation_Report.pdf`. Retrieved on April 15, 2021.

[BC Centre for Disease Control, 2021d] BC Centre for Disease Control (2021d). COVID-19: One Year of the Pandemic in BC. `http://www.bccdc.ca/Health-Info-Site/Documents/CovidBriefing_20210311.pdf`. Retrieved on April 15, 2021.

[Carpenter et al., 2017] Carpenter, B., Gelman, A., Hoffman, M. D., Lee, D., Goodrich, B., Betancourt, M., Brubaker, M., Guo, J., Li, P., Riddell, A., et al. (2017). Stan: A probabilistic programming language. *Journal of Statistical Software*, 76(i01).

[Centres for Disease Control and Prevention, 2021] Centres for Disease Control and Prevention (2021). Pfizer-BioNTech COVID-19 Vaccine Information. `https://www.cdc.gov/vaccines/covid-19/info-by-product/pfizer/index.html`. Retrieved on April 15, 2021.

[Chen and Chen, 2020] Chen, X. and Chen, H. (2020). Differences in Preventive Behaviors of COVID-19 between Urban and Rural Residents: Lessons Learned from A Cross-Sectional Study in China. *International Journal of Environmental Research and Public Health*, 17(12):4437.

[Diekmann et al., 1990] Diekmann, O., Heesterbeek, J., and Metz, J. (1990). On the definition and the computation of the basic reproduction ratio R_0 in models for infectious diseases in heterogeneous populations. *J. Math. Biol.*, 28:365–382.

[Ganyani et al., 2020] Ganyani, T., Kremer, C., Chen, D., Torneri, A., Faes, C., Wallinga, J., and Hens, N. (2020). Estimating the generation interval for coronavirus disease (COVID-19)

based on symptom onset data, March 2020. *Euro surveillance : bulletin Europeen sur les maladies transmissibles*, 25(17):2000257.

[Garasia and Dobbs, 2019] Garasia, S. and Dobbs, G. (2019). Socioeconomic determinants of health and access to health care in rural Canada. *University of Toronto Medical Journal*, 96(2).

[Government of Canada, 2021a] Government of Canada (2021a). Coronavirus disease (COVID-19): Outbreak update. `https://www.canada.ca/en/public-health/services/diseases/2019-novel-coronavirus-infection.html#a`. Retrieved on March 11, 2021.

[Government of Canada, 2021b] Government of Canada (2021b). Vaccines for COVID-19: Shipments and deliveries. `https://www.canada.ca/en/public-health/services/diseases/2019-novel-coronavirus-infection/prevention-risks/covid-19-vaccine-treatment/vaccine-rollout.html`. Retrieved on April 15, 2021.

[Grave et al., 2021] Grave, M., Viguerie, A., Barros, G. F., Reali, A., and Coutinho, A. L. G. A. (2021). Assessing the spatio-temporal spread of COVID-19 via compartmental models with diffusion in Italy, USA, and Brazil. arXiv:2102.07208.

[Hethcote, 2000] Hethcote, H. W. (2000). The Mathematics of Infectious Diseases. *SIAM Review*, 42(4):599–653.

[Interior Health, 2020] Interior Health (2020). Health Authority Profile 2020. `https://www.interiorhealth.ca/AboutUs/QuickFacts/PopulationLocalAreaProfiles/Documents/Interior%20Health%20Authority%20Profile.pdf`. Retrieved on March 31, 2021.

[Korzinski D. and Kurl S., 2020] Korzinski D. and Kurl S. (2020). COVID-19 Carelessness: Which Canadians say pandemic threat is 'overblown'? And how are they behaving in turn? `http://angusreid.org/covid-19-serious-vs-overblown/`. Retrieved on March 12, 2021.

[Lavoie et al., 2016] Lavoie, J. G., Wong, S., Katz, A., and Sinclair, S. (2016). Opportunities and Barriers to Rural, Remote and First Nation Health Services Research in Canada: Comparing Access to Administrative Claims Data in Manitoba and British Columbia. *Healthcare Policy*, 12:1–8.

[Lin et al., 2020] Lin, Q., Zhao, S., Gao, D., Lou, Y., Yang, S., Musa, S. S., and He, D. (2020). A conceptual model for the coronavirus disease 2019 (COVID-19) outbreak in Wuhan, China with individual reaction and governmental action. *International Journal of Infectious Diseases*, 93:211–216.

[Martins N., 2021] Martins N. (2021). CityNews: COVID-19 variant arrives in B.C. `https://www.citynews1130.com/2020/12/27/covid-19-variant-bc/`. Retrieved on April 15, 2021.

[McKee, 2020] McKee, M. (2020). Achieving zero COVID is not easy, but the alternative is far worse. *BMJ.*, 371.

[Migdal A., 2020] Migdal A. (2020). CBCNews: 64-year-old residential care aide is 1st person in B.C. to receive COVID-19 vaccine. `https://www.cbc.ca/news/canada/british-columbia/first-covid-19-vaccine-in-bc-1.5842455`. Retrieved on April 15, 2021.

[OECD, 2020] OECD (2020). *Linking Indigenous Communities with Regional Development in Canada*. OECD Publishing, Paris.

[Overton et al., 2020] Overton, C. E., Stage, H. B., Ahmad, S., Curran-Sebastian, J., Dark, P., Das, R., Fearon, E., Felton, T., Fyles, M., Gent, N., Hall, I., House, T., Lewkowicz, H., Pang, X., Pellis, L., Sawko, R., Ustianowski, A., Vekaria, B., and Webb, L. (2020). Using statistics and mathematical modelling to understand infectious disease outbreaks: COVID-19 as an example. *Infectious Disease Modelling*, 5:409–441.

[Shafer et al., 2021] Shafer, L. A., Nesca, M., and Balshaw, R. (2021). Relaxation of social distancing restrictions: Model estimated impact on COVID-19 epidemic in Manitoba, Canada. *PLOS ONE*, 16(1):1–15.

[The Canadian Press, 2021] The Canadian Press (2021). Coronavirus: Here's a timeline of COVID-19 cases in Canada. `https://globalnews.ca/news/6627505/coronavirus-covid-canada-timeline/`. Retrieved on March 12, 2021.

[Tindale et al., 2020] Tindale, L. C., Stockdale, J. E., Coombe, M., Garlock, E. S., Lau, W. Y. V., Saraswat, M., Zhang, L., Chen, D., Wallinga, J., and Colijn, C. (2020). Evidence for transmission of COVID-19 prior to symptom onset. *eLife*, 9:e57149.

[Tuite et al., 2020] Tuite, A. R., Fisman, D. N., and Greer, A. L. (2020). Mathematical modelling of COVID-19 transmission and mitigation strategies in the population of Ontario, Canada. *CMAJ*, 192(19):E497–E505.

[Turk et al., 2020] Turk, P. J., Chou, S.-H., Kowalkowski, M. A., Palmer, P. P., Priem, J. S., D., S. M., J., T. Y., and McWilliams, A. D. (2020). Modeling COVID-19 Latent Prevalence to Assess a Public Health Intervention at a State and Regional Scale: Retrospective Cohort Study. *JMIR Public Health Surveill.*, 6(2):19353.

[van den Driessche and Watmough, 2002] van den Driessche, P. and Watmough, J. (2002). Reproduction numbers and sub-threshold endemic equilibria for compartmental models of disease transmission. *Mathematical Biosciences*, 180(1):29–48.

[Youssef et al., 2020] Youssef, H. M., Alghamdi, N. A., Ezzat, M. A., El-Bary, A. A., and Shawky, A. M. (2020). A modified SEIR model applied to the data of COVID-19 spread in Saudi Arabia. *AIP Advances*, 10(12):125210.

Appendix A Trace plots

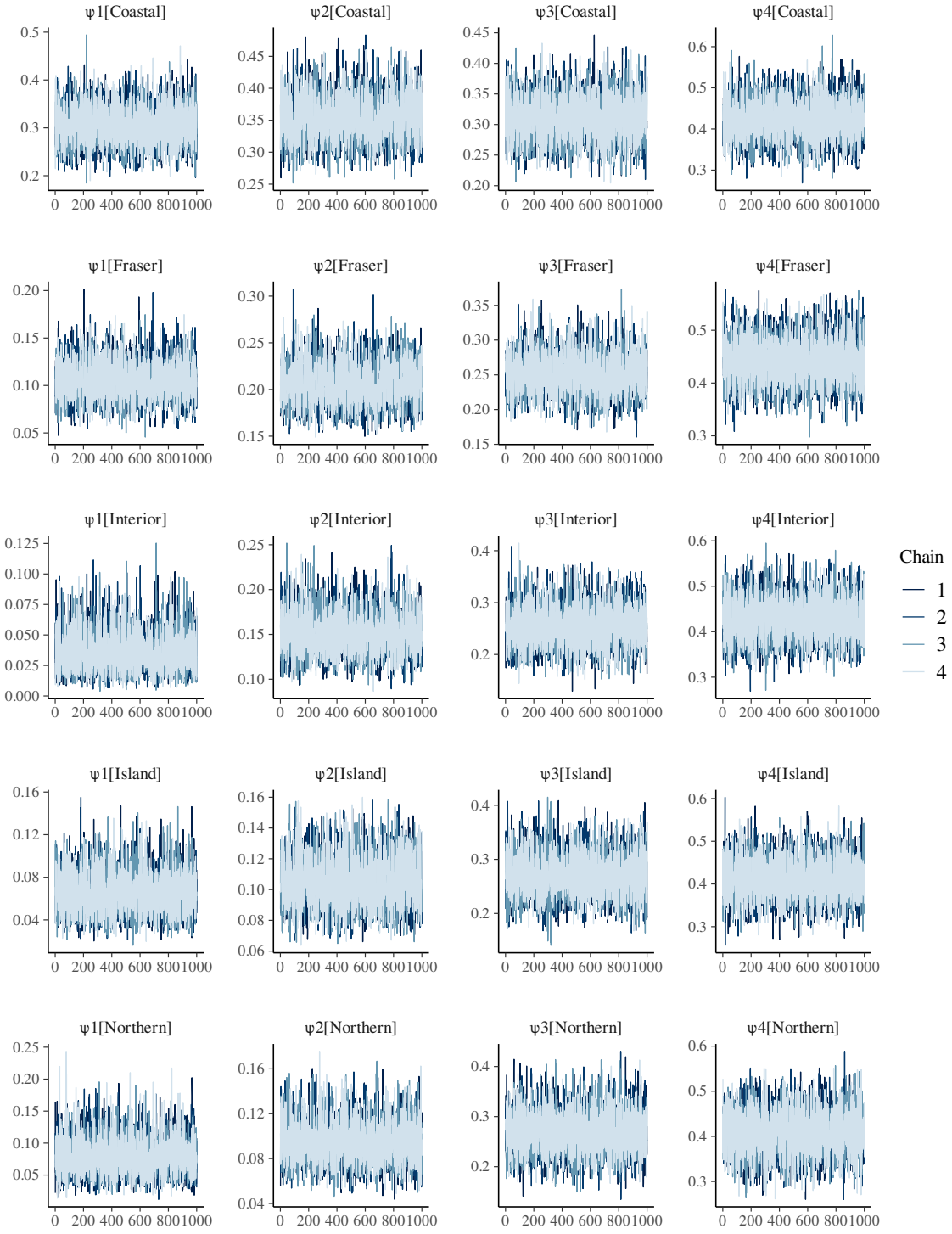

Figure 8: Trace plots of runs for the regional $\psi_1, \ldots, \psi_4$.

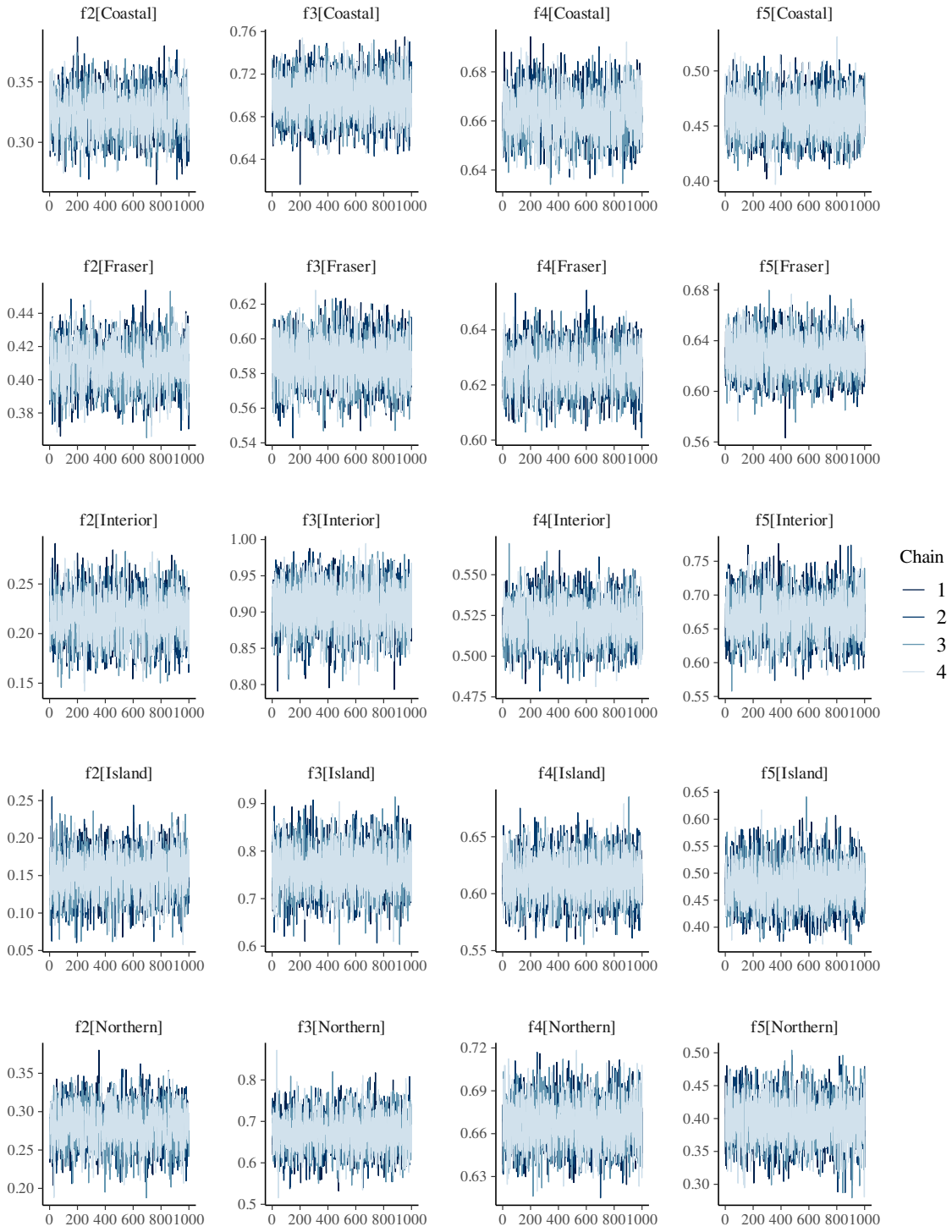

Figure 9: Trace plots of runs for the regional $f_2, \ldots, f_5$.

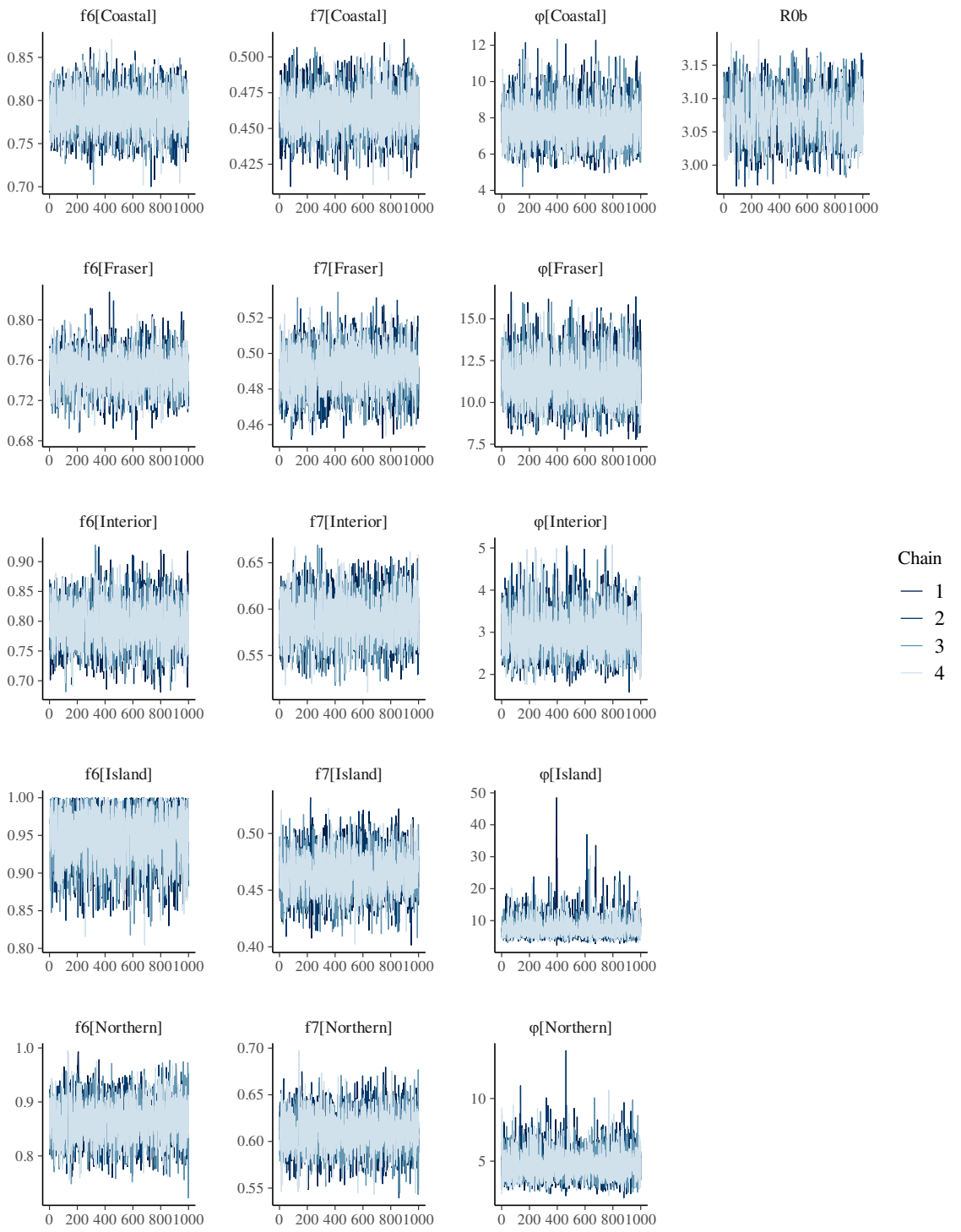

Figure 10: Trace plots of runs for the regional f_6, f_7, ϕ and hierarchical regional R_{0b}.

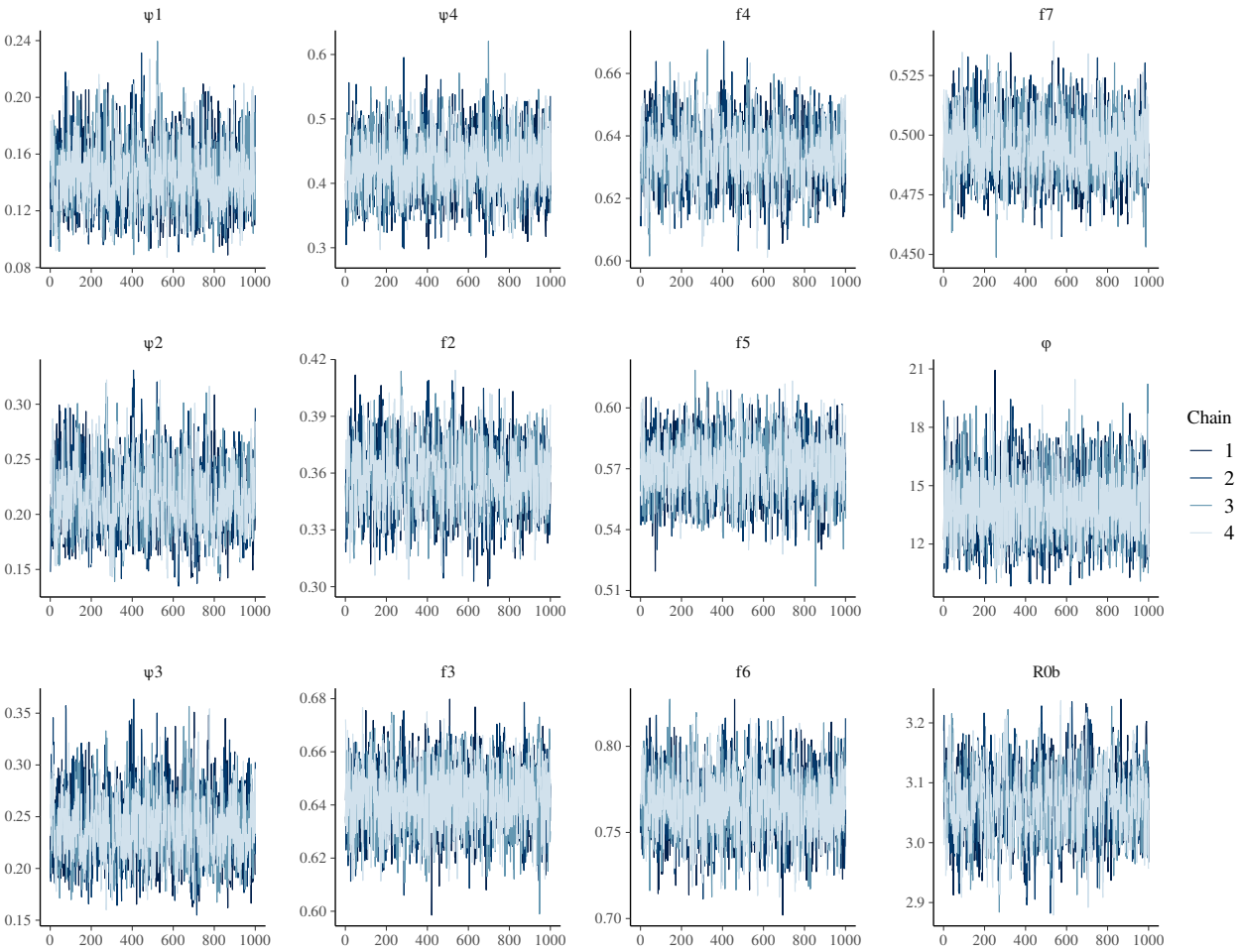

Figure 11: Trace plots of runs for the provincial-wide $\psi_1, \ldots, \psi_4, f_2, \ldots, f_7, \phi, R_{0b}$.